SEL EXHIBIT NO. 2014

INNOLUX CORP. v. PATENT OF SEMICONDUCTOR ENERGY LABORATORY CO., LTD.

IPR2013-00064

Microsystem Technologies 10 (2004) 603–607 © Springer-Verlag 2004
DOI 10.1007/s00542-003-0338-3

Anisotropic Si deep beam etching with profile control using SF_6/O_2 Plasma

H. Zou

Abstract This paper presents the results of dry plasma etching of single crystal silicon using SF_6 and O_2 as process gases in a traditional Reactive Ion Etcher. The highly anisotropic profiles are achieved for a deep beam feature with depths in excess of 100 μm. The effect of O_2 concentration on both etch rate and etch profile is investigated across a range of chamber pressures. Etch profile anisotropy can be controlled through appropriate variations in O_2 and SF_6 flow rate and SEM images are provided to show this effect over a range of chamber pressures and RF powers. Our results indicate O_2 concentration to be the primary factor influencing etch profile, while system pressure is shown to have a strong influence over etch rate. Shadowing effect also has been discussed for the possible application of releasing the freestanding beams. These results aided in the formulation of a suitable process for fabricating long-travel electrothermally actuated beam structures with the depth and width of 100 μm and 20 μm. The ratio of beam depth to the mask-undercut is 10:1. This etching technique is resulting in the successful fabrication of thermoelectrically-driven long-travel beam structures.

1
Introduction

An important factor in any silicon etch process is the ability to control the profile of the etch cavity. In the fabrication of MEMS sensors and actuators, vertical walls are especially desirable [1–4]. Reactive ion etching (RIE) is a popular choice for etching silicon; here, fluoride-based plasmas are used because of their ability to spontaneously react with silicon at room temperature to create isotropic etch features. Anisotropic etching and high etch rates have been demonstrated in RIE plasmas containing SF_6 and O_2 [5–8].

In our investigation, SF_6 and O_2 are chosen for RIE etching of silicon. In a plasma containing SF_6 and O_2, each gas has its own specific function, so by altering the flow rate of one of the gases, changes to the etch profile can be achieved. The SF_6 and O_2 generate F^* and O^* free-radicals under the influence of strong electric fields generated in the reactive ion etcher. The F^* radicals initiate a chemical reaction with silicon, producing the highly volatile by-product SiF_4. The O^* radicals act to passivate the silicon surface by forming SiO_xF_y (siliconoxyfluoride). In addition to generating F^* radicals, SF_6 is also the source of SF_X^+ ions, which act to remove the oxyfluoride layer. Alternate formation and removal of the oxyfluoride layer is the enabling mechanism behind anisotropic etching of silicon [9–12].

Substrate damage and mask erosion can be minimised through appropriate lowering of ion energy. Etch profile is also more controllable at lower ion energies. Ion energy is governed by the dark space voltage, Dv, which is the potential developed between the plasma and the powered electrode. The O_2 creates high voltages, whereas SF_6 results in lower voltages. The Dv voltage also increases with increasing input power, R_{RF} and decreasing system pressure, p. The relationship can be expressed qualitatively as [13]:

$$\mathrm{Dv} \ \alpha \frac{P_{RF} \cdot F[O_2]}{p \cdot F[SF_6]} \tag{1}$$

where F[gas] refers to the gas flow rate. The dark space voltage is not easily measured. In practice DC bias is measured instead, as this is known to increase with increasing dark space voltage [9]. In the etching of silicon using the SF_6/O_2 mixture, there is a continual competition between etching and passivating reactions caused by $F^\cdot$ and $O^\cdot$ free-radicals, respectively. When RF power, system pressure and gas flow rates are at the right levels, etch features with vertical side walls result.

2
Experimental

Etching trials were conducted using an Oxford Instruments PlasmaLab 80+ reactive ion etcher. Figure 1 shows the key components featured in the etcher.

The PlasmaLab 80+ consists of a pair of parallel plate electrodes connected to a 13.56 MHz RF generator, capable of automatic matching. The base-plate electrode is 20 cm in diameter and is water-cooled, allowing an adjustable temperature range of 5–20 °C. Base-plate temperature was maintained at 20 °C for all experiments.

Received: 17 April 2003 / Accepted: 9 September 2003

H. Zou
Optical and Semiconductor Devices Group,
Department of Electrical and Electronic Engineering,
Imperial College London, Exhibition Road,
London SW7 2BT, UK
e-mail: h.zou@imperial.ac.uk

The author would like to thank Professor R. R. A. Syms and Mr Michael Larsson for encouraging and useful discussions during this work. This project is supported by the EPSRC under grant GR/R07844/01.

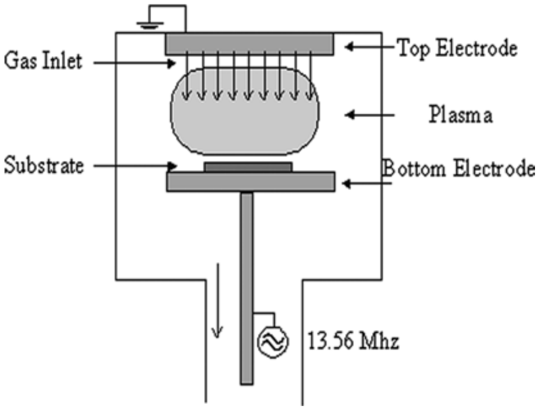

Fig. 1. RIE PlasmaLab 80+ component layout

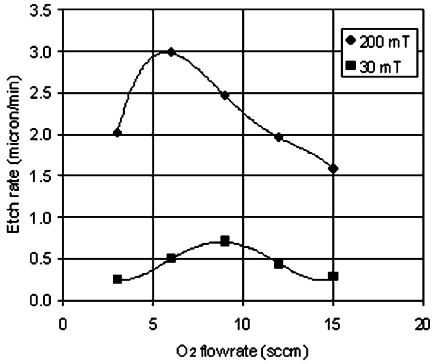

Fig. 2. Si etch rate dependency on O_2 flow rate: 12 sccm SF_6 at 160 W RF power, with DC bias varying from 360 to 387 V at 30 mTorr and from 117 to 175 V at 200 mTorr

Gas-flows are controlled by a standard mass-flow regulator and mixed prior to entering the chamber via the gas inlet.

Etch profile is investigated by sectioning samples and viewing in a scanning electron microscope (SEM). Measurements of etch depth and lateral etch of the vertical face beneath the mask layer are made using the SEM.

All samples used originate from 4-inch <100> oriented, phosphorous-doped single crystal silicon wafers, with resistivity within the range 1–10 Ωcm. The etch mask used is 2000 Å thick chromium, applied via sputtering. Patterning of the chromium layer is achieved using a 1.3 μm layer of Shipley S1813 positive-working photoresist, which is itself patterned using standard photolithography processes. Sample sizes were approximately 3.5 cm^2 in area, and a dummy 4-inch wafer was employed to maintain loading consistency between trials.

3
Results and discussions

Oxygen concentration

The effect of oxygen concentration on etch rate and profile has been investigated. Keeping the SF_6 flow rate and substrate electrode temperature constant, the system pressure is set at 30 and 200 mTorr, respectively. The effect of increments in oxygen concentration on etch rate and etch profile is demonstrated in Figs. 2 and 3, respectively.

Figure 2 indicates an increase in silicon etch rate up to a maximum, followed by a decrease, with increasing oxygen flow rate. The maximum etch rate with system pressure set to 200 mTorr is approximately twice that of the minimum value. In addition, the etch rate is greater when system pressure is at 200 mTorr rather than 30 mTorr.

At low oxygen concentrations, further increments of oxygen have the effect of facilitating the conversion of SF_6 to F^* radicals, as the oxygen reacts with fluorosulphur radicals, thereby hindering their reaction with F^* radicals and the subsequent re-formation of sulphur hexafluoride (SF_6). The result is a net increase in the concentration of fluoride radicals, leading to an increase in the silicon etch rate. At high oxygen concentrations, however, there is competition between the F^* and O^* radicals for reaction with silicon; the former resulting in etching, the latter resulting in surface passivation. At very high oxygen concentrations, the silicon etch rate is retarded due to polymerisation on the side walls and bases of etch trenches. The polymers protect the silicon from reaction with F^* radicals, thereby, causing a decrease in silicon etch rate with further increases in oxygen concentration [9, 12].

The effect of oxygen concentration on silicon etch profile is shown in Fig. 3. The SF_6 flow rate and system pressure are kept constant at 12 sccm and 200 mTorr, respectively. At an oxygen flow rate of 4 sccm (Fig. 3a), the silicon etch profile is largely isotropic (i.e. non-directional). At a flow rate of 6 sccm (Fig. 3b), the degree of

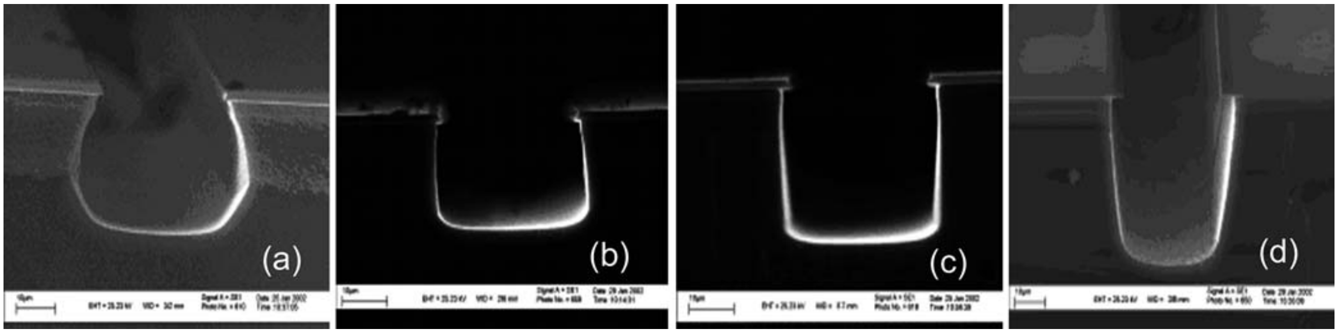

Fig. 3. SEM cross section micrographs of 30 μm wide trenches etched at different O_2 flow rates of **a** 4 sccm, **b** 6 sccm, **c** 9 sccm, **d** 12 sccm respectively. Other conditions: SF_6: 12 sccm; system pressure: 200 mTorr, RF power: 160 W

isotropy is reduced, and the side-wall profile can best be described as following a negative taper. At an oxygen flow rate of 9 sccm (Fig. 3c), side-walls exhibit a dual positive-negative taper, with the overall result close to 90° with respect to the horizontal. Finally, at an oxygen flow rate of 12 sccm, the side-walls exhibit a positive taper and the base of the etch trench becomes rounded (Fig. 3d).

System pressure

Silicon etch rate is found to be strongly dependent upon system pressure; this is shown in Fig. 4. The SF_6 and O_2 flow rates are kept constant at 12 sccm and 7 sccm, respectively and RF power maintained at 200 W. System pressure is varied between 150 mTorr and 200 mTorr. A monotonic increase in silicon etch rate is observed with increasing system pressure until a pressure of 180 mTorr, after which the silicon etch rate continues to increase, but at a lower rate. A maximum etch rate of approximately 880 nm/min is reached at a system pressure of 200 mTorr. The increase in etch rate with system pressure is directly attributable to the increase in plasma ion density resulting from increasing system pressure.

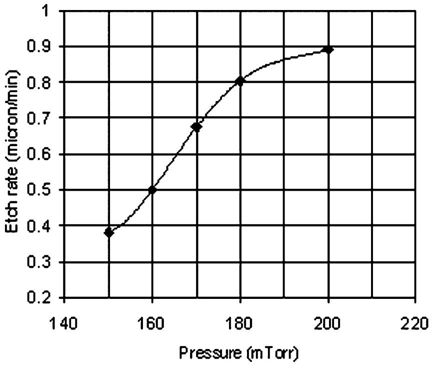

Fig. 4. Si etch rate as a function of system pressure: 2 sccm SF_6, 7 sccm O_2 at 200 W RF input power, with DC bias varying from 223 to 167 V

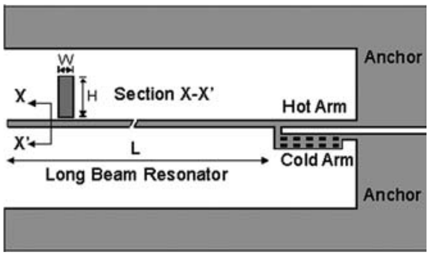

Fig. 5. Layout of electrothermally driven, long-travel beam resonator

Anisotropic etching of the long-travel beam resonator

The layout of an electrothermally-driven, long-travel beam resonator [3] is shown in Fig. 5. The intention is to fabricate the device using deep anisotropic reactive ion etching. The design in question has dimensions L = 14 mm, W = 25 μm and H = 100 μm.

The device is fabricated from a <100> oriented single crystal silicon wafer. A 2000 Å thick chromium etch-mask was applied via sputtering. Release of the long-travel beams is to be achieved via a final isotropic etch step.

Figure 6 shows SEM images of beam-tips to illustrate the variation in anisotropy achieved at various oxygen flow rates, and the details of the processing parameters are summarized in Table 1. Figure 6a, b and c indicate the influence of an increase in oxygen flow rate on the etched profiles with the fixed SF_6 flow rate, RF power and system pressure. An anisotropic profile can be obtained at an oxygen flow rate of 8 sccm (Fig. 6b). However oxygen flow rates of 5 sccm and 10 sccm, either side of this critical point, lead to worsening of beam profile; with either negative taper (Fig. 6a) or positive taper (Fig. 6c), respectively.

Comparison of Fig. 6d and 6e show the effect of a decrease in system pressure from 200 mTorr to 160 mTorr on etch profile. It can be seen that the decrease in system pressure (all other process parameters remaining constant) results in a decrease in lateral etch in the region of side-wall directly beneath the etch mask; the reduction is from 11 μm to 8 μm. A reason for this observed decrease stems from the fact that at lower system pressures, fewer reactive ions exist within the chamber at any one time, resulting in fewer collisions and fewer chances for poorly directed ions to cause lateral etching.

Figure 7 shows an isometric view of a long-travel beam resonator, formed via anisotropic reactive ion etching; etching parameters being 12 sccm SF_6, 7 sccm O_2, 200 W RF power and 160 mTorr's of system pressure. The depth and

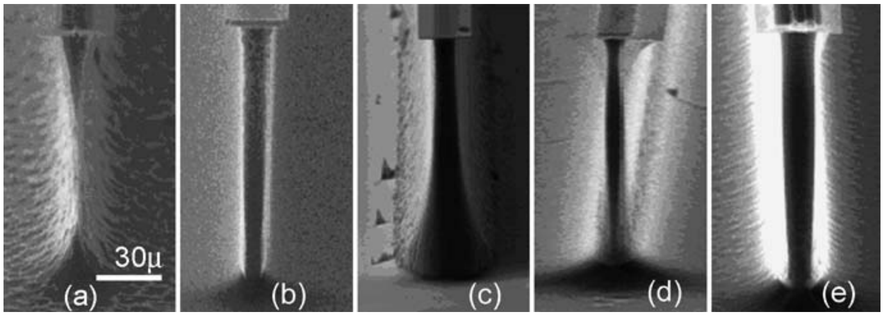

Fig. 6. Variations in etch profile with various O_2 flow rates **a** 5 sccm, **b** 8 sccm, **c** 10 sccm; other parameters, SF_6 12 sccm, RF power 200 W, system pressure 160 mTorr. SEM images showing anisotropic etching with different system pressure, **d** 200 mTorr, **e** 160 mTorr. Other parameters; SF_6 12 sccm, RF power 200 W, O_2 7 sccm

Table 1. Processing parameters for anisotropic etching of long, narrow and deep beam

Samples	SF_6 flow (sccm)	O_2 flow (sccm)	RF Power (W)	Pressure (mTorr)	Beam depth (µm)	Mask-undercut (µm)
(a)	12	5	200	160	100	10
(b)	12	8	200	160	95	8
(c)	12	10	200	160	115	9
(d)	12	7	200	200	110	11
(e)	12	7	200	160	105	8

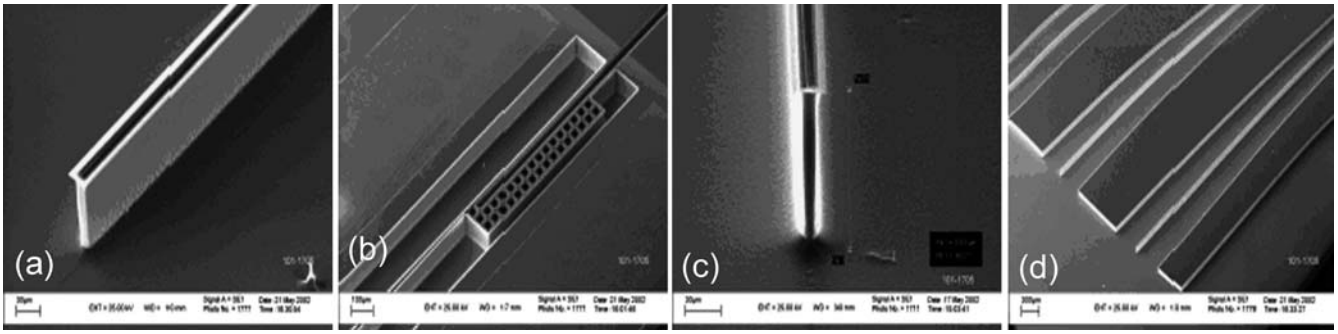

Fig. 7. Isometric view of long-beam resonator structure after isotropic etching, showing beam profiles **a**, **c** and **d** and electrothermal actuator **b**. Etch conditions: SF_6 12 sccm, O_2 7 sccm, RF power 200 W, system pressure 160 mTorr

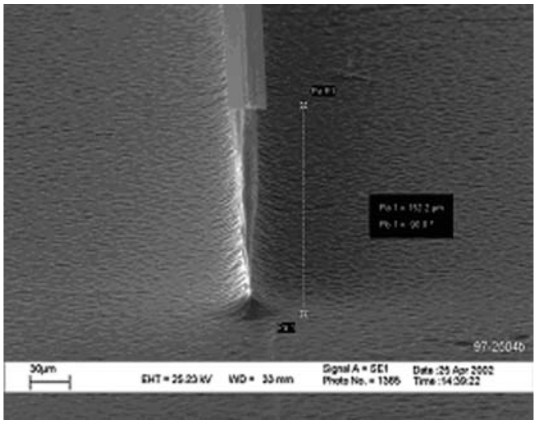

Fig. 8. Free-standing beam with negatively sloped sidewalls etched by ions at angles-of-incidence deviating from the vertical direction

width of the beam are 105 µm and 20 µm, respectively. The ratio of beam depth to the mask-undercut is 10:1. The cantilever beams were released using SCREAM processing [14]. After anisotropic etching the freestanding beams were released by isotropic etching of the SF_6 plasma.

Shadowing effect

Ions with an angle-of-incidence substantially different to the vertical are prevented from proceeding along their intended path by the sidewalls of narrow trenches and / or nearby free-standing features; the effect is known as 'shadowing'. Shadowing of ions by beam or trench sidewalls is one reason for the decrease in etch-rate that is observed with increasing feature aspect ratio, known as RIE-lag [15–17], if the etch rate is substantially governed by ion assistance.

Free-standing features, such as single lines or walls, which are subject to ion bombardment at angles-of-incidence deviating from the vertical, will eventually assume a negative taper. Such an effect can be used to under etch free-standing beams with negatively sloping side walls that eventually meet on the underside (Fig. 8).

4
Conclusions

The anisotropic etching of single crystal silicon using SF_6 and O_2 process gas mixtures has been demonstrated using a PlasmaLab 80+ RIE system. Our results suggest O_2 concentration to be the principal factor influencing etch profile, while etch rate is strongly affected by system pressure. Based on these findings, process recipes were developed to achieve anisotropic profiles for fabricating deep beams with the depth and width of 100 µm and 20 µm. The ratio of beam depth to the mask-undercut is 10:1. This etching technique allowed the successful fabrication of thermoelectrically-driven long-travel beam structures.

References

1. **Syms RRA; Moore DF** (2002) Optical MEMS for telecommunications. Materials Today July/August Issue: 26–35
2. **Syms RRA; Lohmann A** (2002) A Tuning mechanism for a MEMS external cavity laser. Proceedings of IEEE/LEOS International Conference on Optical MEMS and their Applications, Lugano, Switzerland, 20–23 August: paper ThD4
3. **Syms RRA** (2002) Long-travel electrothermally-driven resonant cantilever microactuators. J Micromech Microeng 12: 211–218
4. **Jansen HV; de Boer MJ** (1996) High aspect ratio trench etching for MEMS applications. Proceedings of IEEE The Ninth Annual International workshop Micro Electrical Mechanical System, San Diego, USA, pp. 250–257

DOCKET ALARM

Explore Litigation Insights

Docket Alarm provides insights to develop a more informed litigation strategy and the peace of mind of knowing you're on top of things.

Real-Time Litigation Alerts

Keep your litigation team up-to-date with **real-time alerts** and advanced team management tools built for the enterprise, all while greatly reducing PACER spend.

Our comprehensive service means we can handle Federal, State, and Administrative courts across the country.

Advanced Docket Research

With over 230 million records, Docket Alarm's cloud-native docket research platform finds what other services can't. Coverage includes Federal, State, plus PTAB, TTAB, ITC and NLRB decisions, all in one place.

Identify arguments that have been successful in the past with full text, pinpoint searching. Link to case law cited within any court document via Fastcase.

Analytics At Your Fingertips

Learn what happened the last time a particular judge, opposing counsel or company faced cases similar to yours.

Advanced out-of-the-box PTAB and TTAB analytics are always at your fingertips.

API

Docket Alarm offers a powerful API (application programming interface) to developers that want to integrate case filings into their apps.

LAW FIRMS

Build custom dashboards for your attorneys and clients with live data direct from the court.

Automate many repetitive legal tasks like conflict checks, document management, and marketing.

FINANCIAL INSTITUTIONS

Litigation and bankruptcy checks for companies and debtors.

E-DISCOVERY AND LEGAL VENDORS

Sync your system to PACER to automate legal marketing.

WHAT WILL YOU BUILD? | **sales@docketalarm.com** | **1-866-77-FASTCASE**

fastcase®
Smarter legal research.